Experimental Thermal and Fluid Science 35 (2011) 636–644

Contents lists available at ScienceDirect

Experimental Thermal and Fluid Science

journal homepage: www.elsevier.com/locate/etfs

Flow boiling heat transfer and pressure drop of R-134a in a mini tube: an experimental investigation

Jacqueline B. Copetti *, Mario H. Macagnan, Flávia Zinani, Nicole L.F. Kunsler

Mechanical Engineering Graduate Program, Universidade do Vale do Rio dos Sinos, UNISINOS, Av. Unisinos 950, 93022.000, São Leopoldo, RS, Brazil

ARTICLE INFO

Article history:
Received 23 August 2010
Received in revised form 21 December 2010
Accepted 21 December 2010
Available online 30 December 2010

Keywords:
Flow boiling
Mini channels
Heat transfer coefficients
Pressure drop
R-134a

ABSTRACT

This paper presents the results of an experimental study carried out with R-134a during flow boiling in a horizontal tube of 2.6 mm ID. The experimental tests included (i) heat fluxes in the range from 10 to 100 kW/m^2, (ii) the refrigerant mass velocities set to the discrete values in the range of 240–930 kg/(m^2 s) and (iii) saturation temperature of 12 and 22 °C. The study analyzed the heat transfer, through the local heat transfer coefficient along of flow, and pressure drop, under the variation of these different parameters. It was possible to observe the significant influence of heat flux in the heat transfer coefficient and mass velocity in the pressure drop, besides the effects of saturation temperature. In the low quality region, it was possible to observe a significant influence of heat flux on the heat transfer coefficient. In the high vapor quality region, for high mass velocities, this influence tended to vanish, and the coefficient decreased. The influence of mass velocity in the heat transfer coefficient was detected in most tests for a threshold value of vapor quality, which was higher as the heat flux increased. For higher heat flux the heat transfer coefficient was nearly independent of mass velocity. The frictional pressure drop increased with the increase in vapor quality and mass velocity. Predictive models for heat transfer coefficient in mini channels were evaluated and the calculated coefficient agreed well with measured data within a range 35% for saturation temperature of 22 °C. These results extend the ranges of heat fluxes and mass velocities beyond values available in literature, and add a substantial contribution to the comprehension of boiling heat transfer phenomena inside mini channels.

1. Introduction

Flow boiling studies in mini and micro channels have been published, mainly in the last two decades, motivated by the current trend to develop innovative compact systems in applications such as refrigeration systems, high heat flux cooling and cooling of electronic devices.

Most researchers from the available literature, point out a great increment in heat transfer achieved by small diameter channels when comparing to usual ones. Meanwhile, most of the published results present discrepancies concerning the effect of heat flux, mass velocity and saturation temperature on the value of the heat transfer coefficient.

The characteristics and mechanisms of flow boiling in mini and micro channels are not completely understood yet, and are a controversial point in the literature. According to published results, boiling heat transfer could be controlled by nucleate boiling, due to nearly exclusively dependency on heat flux [1,2], or by convective boiling, with the dependence of mass flux and vapor quality [3] or by both, depending on vapor quality range [4,5]. Moreover, some authors [6,7] claim that nucleate boiling is not the dominant heat transfer mechanism, but the transient evaporation of a thin liquid film around elongated bubbles.

The definition of such dependence and, consequently, the capability of heat transfer prediction under any of these conditions through the correlations is limited, but it has been the main goal of several researchers in this area [7–12].

Some observations from different experiments are summarized in the next paragraphs.

Tran et al. [1] studied R-12 in a 2.46 mm circular tube and observed the heat transfer dependence on heat flux, but the effects of mass velocity and vapor quality were negligible. The same tendency was reported by Lazarek and Black [2] and Wambsganss et al. [13] with R-113 boiling in a 3.1 mm and 2.92 mm tubes, respectively. However, the results shown by Yan and Lin [4], Lin et al. [5] and Choi et al. [14] demonstrated that the effects of mass velocity and vapor quality also are important.

The heat transfer coefficients obtained from experiments carried out by Lin, et al. [5] with R-141b in 1.3–3.69 mm channels showed that heat flux is important only in the low quality region ($X < 0.4$) and the heat transfer coefficient increases with the

* Corresponding author.
E-mail address: jcopetti@unisinos.br (J.B. Copetti).

0894-1777
doi:10.1016/j.expthermflusci.2010.12.013

Nomenclature

dh_{max} heat transfer coefficient maximum uncertainty (–)
dp/dz local pressure drop (kPa/m)
$(dp/dz)_f$ frictional pressure drop (kPa/m)
G mass velocity (kg/(m^2 s))
h heat transfer coefficient (W/(m^2 K))
h_{exp} experimental heat transfer coefficient (W/(m^2 K))
h_{pred} predicted heat transfer coefficient (W/(m^2 K))
i_f liquid enthalpy (kJ/kg)
i_{fg} latent heat of vaporization (kJ/kg)
$i_{i\text{-}TS}$ test section inlet enthalpy (kJ/kg)
$i_{i\text{-}PH}$ pre-heater inlet enthalpy (kJ/kg)
k thermal conductivity (W/(m K))
$\dot{m}$ mass flow rate (kg/s)
$\mathrm{MBE} = \frac{1}{n}\sum_{i=1}^{n}\frac{h_{pred_i}-h_{exp_i}}{h_{exp_i}} \times 100$ mean bias error (%)
P electrical power input (W)
q'' heat flux (kW/m^2)
$\dot{q}$ volumetric heat generated (W/m^3)
q_{PH} pre-heater heat rate (W)
r_i internal radius (m)
r_o external radius (m)
$\mathrm{RMSE} = \sqrt{\frac{1}{n}\sum_{i=1}^{n}\left(\frac{h_{pred_i}-h_{exp_i}}{h_{exp_i}}\right)^2} \times 100$ root mean square error (%)
T_{sat} saturation temperature (°C)
$T_{w,i}$ internal wall temperature (°C)
$T_{w,o}$ external wall temperature (°C)
$T_{w,botton}$ external wall bottom temperature (°C)
$T_{w,side\_inner}$ external wall inside temperature (°C)
$T_{w,side\_outer}$ external wall outside temperature (°C)
$T_{w,top}$ external wall top temperature (°C)
X vapor quality (–)
$X_{i\text{-}TS}$ vapor quality in the entrance of test section (–)
η heat transfer efficiency (–)
η_{PH} pre-heater heat exchange efficiency (–)
η_{TS} test section heat exchange efficiency (–)

increase in vapor quality until a point when the coefficient decreases gradually, but the inflection point in the vapor quality range is also heat flux dependent.

Saitoh et al. [15] analyzed the effect of tube diameter on boiling heat transfer of R-134a with heat fluxes in the range of 5–39 kW/m^2 and mass velocities between 150 and 450 kg/(m^2 s). For a 3.1 mm diameter tube they found a clear dependency of the heat transfer coefficient on both heat and mass flux, unlike for the 0.51 mm tube, where they observed the effect of heat flux only. These authors suggested that the contribution of forced convection to the boiling heat transfer decreases with decreasing tube diameter. Moreover, these authors observed that the pressure drop for small diameter tubes was better predicted by the homogeneous model than by the Lockhart–Martinelli correlation [16], suggesting that, as the tube diameter decreases, the flow in the liquid phase approaches laminar flow and the effect of forced convective boiling is suppressed.

In the same way, Shiferaw et al. [9] studied the refrigerant R-134a and channel diameters from 2.01 mm to 4.26 mm and found similar results. In the experiments with the 4.26 mm tube, the heat transfer coefficient increased with heat flux and saturation temperature, but it remained constant in the vapor quality range from 0.4 to 0.5 in low heat fluxes. For the 2.01 mm tube, this range moved down to 0.2–0.3 of vapor quality.

Choi et al. [14] investigated flow boiling of R-22, R-134a and CO_2 in tubes of 1.5 and 3.0 mm, employing heat fluxes from 10 to 40 kW/m^2 and mass velocities from 200 to 600 kg/(m^2 s). They observed an increase in the heat transfer coefficient with the increase in vapor quality, and also a heat flux dependence. This increase is followed by a decrease which occurs at lower qualities for higher mass velocities. In the high quality region, the heat transfer coefficient was predominantly dependent on mass velocity.

In the paper by Choi et al. [14], as in many others, the dependence of heat transfer coefficient on heat flux is interpreted as evidence that nucleate boiling is the dominant heat transfer mechanism at low quality region. Also, in the high vapor quality range, when the heat transfer coefficient becomes independent of heat flux and decreases with quality, it is claimed to indicate predominance of the convective mechanism. Most authors also verify the minor influence of mass velocity on the heat transfer coefficient with the reduction of channel diameter, associating this behavior to the decreasing of convective contribution, which is characteristic of macro channels. Moreover, some effects, like the dryout, could happen in lower vapor qualities in micro channels, as a result of confinement and the increasing relevance of surface tension, thus justifying the increase of the nucleate boiling contribution.

Jacobi and Thome [6] and Thome et al. [7], demonstrated through the two and three-zone flow boiling heat transfer models, that the dependence of the heat transfer coefficient on the heat flux is not necessarily associated with nucleate boiling, but to the evaporation of a thin liquid film around the bubbles which causes the coefficient increases as heat flux increases.

More recently, Tibiriçá and Ribatski [17] and Ong and Thome [18], presented a comprehensive study of the flow boiling in small tubes for different refrigerants, including the R-134a. The first work examined the influence of mass velocity from 100 to 700 kg/(m^2 s) and heat flux from 5 to 35 kW/m^2 and the authors found that the heat transfer coefficient increased with the mass velocity and vapor quality except for mass velocities below a threshold of 200 kg/(m^2 s), which experimented a premature and smooth decrease with increasing vapor quality. Also, the heat transfer coefficient increased with heat flux independently of the fluid or mass velocity range. In the second work [18], the heat transfer coefficient behavior for different refrigerants was associated to flow regime transition for different vapor qualities. They concluded that convective boiling seems to dominate at higher vapor qualities in the annular flow, and in the bubbly regime, at low vapor qualities, the heat transfer coefficient depends on heat flux. However, it is difficult to separate the patterns. As the mass velocity increases the transition to annular flow occurs at lower qualities.

Associated with lack of the phenomenon understanding to explain the observed trends and consequently the importance of nucleate and convective boiling contributions, is the difficulty to carry out two-phase flow experiments in small sizes tubes. According to Consolini [8], the experiments are very sensitive to instabilities that are possibly responsible for variations in the results of different studies.

The present paper aims to provide experimental results in a broader operational range and add a contribution to the comprehension of boiling heat transfer phenomena inside mini channels. The experimental results of R-134a flow boiling through a stainless

steel mini channel of 2.62 mm ID are reported. The heat transfer coefficient and pressure drop were investigated with respect to changes in vapor quality, heat flux and mass velocity. Moreover, the experimental results were compared with several available flow boiling predictive methods for heat transfer coefficient and pressure drop.

2. Experimental aspects

2.1. Facility and instrumentation

An experimental facility was developed to investigate flow boiling and pressure drop in electrically heated horizontal mini channels. The details of this facility are shown schematically in Fig. 1. The experimental system consists of a loop that provides controlled mass velocity, and it was designed to test different fluids at a wide range of flow conditions. The main part of the loop has a Coriolis mass flow meter, a pre-heater section, the test section and the visualization section.

The secondary part consists of a condenser, a refrigerant reservoir, a dryer filter, a liquid refrigerant vessel, a volumetric pump and a subcooler. The condenser and the subcooler have independent circuits, each uses an ethylene–glycol/water solution as secondary refrigerant, which temperature is controlled by a thermostatic bath. The liquid refrigerant vessel (approximately 1 L) is placed upstream the pump and filled with liquid refrigerant, in order to maintain a constant static pressure at the pump suction. This procedure assures that the pump works uniformly and drowned, avoiding cavitation. The subcooler is placed downstream the pump, upstream the flow meter. The subcooler is used to compensate any temperature rise which usually occurs as the refrigerant passes the gear pump, and also to assure that only subcooled liquid enters the flow meter. The refrigerant reservoir connected to the main circuit of the bench, as shown in Fig. 1, operates as a pressure regulator, maintaining stable conditions during the experiments.

The pre-heater establishes the experimental conditions entering the test section just downstream. It consists of a horizontal cooper tube with length of 445 mm heated by an electrical tape resistance (11.7 Ω/m) uniformly wrapped around its external surface to guarantee a uniform heat flux to the refrigerant. The electrical resistance is electrically insulated from the tube with a Kapton conductive tape. In the pre-heater, power is adjusted by a voltage converter.

The test section consists of a smooth horizontal stainless steel tube with effective length of 183 mm and 2.62 mm ID. This tube is uniformly heated by direct application of electrical current in the tube wall (Joule effect), which intensity is controlled by the power supply. The absolute internal roughness (Ra) of the tube was measured with a Pantec roughness tester, and is of 2.05 μm. Downstream the test section there is a visualization section with a 158 mm length glass tube with the same test section internal diameter.

Both the pre-heater and test section are thermally insulated using a fiberglass cover, reducing heat losses to the surroundings.

The refrigerant enters the pre-heater in the condition of subcooled liquid and achieves the saturation condition upstream its outlet. This condition defines the vapor quality in the test section inlet, and varies according to the heat flux imposed in the pre-heater. The pressure and temperature measurements in the inlet and outlet of the pre-heater are carried out by two absolute pressure transducers and two 0.076 mm thermocouples of type E, in direct contact with the refrigerant.

Refrigerant temperatures are measured in the inlet and outlet of test section, as well as the tube wall temperatures. The tube wall thermocouples are type E of 0.076 mm directly fixed by a thermally conductive paste. The position of each thermocouple is shown in Fig. 1. In the three central axial positions of the tube there are four thermocouples per position, separated by 90° one of the other. In the entrance and exit of the tube are fixed two thermocouples on the wall, in the upper and bottom parts. The differential pressure transducer allows the determination of the outlet pressure.

The pump flow rate is controlled by a frequency inverter and a bypass line downstream the pump, controlled by a needle-valve, is used to set precise flow rates.

The pressure transducers, thermocouples, mass flow and power meter were connected to an acquisition data system composed by

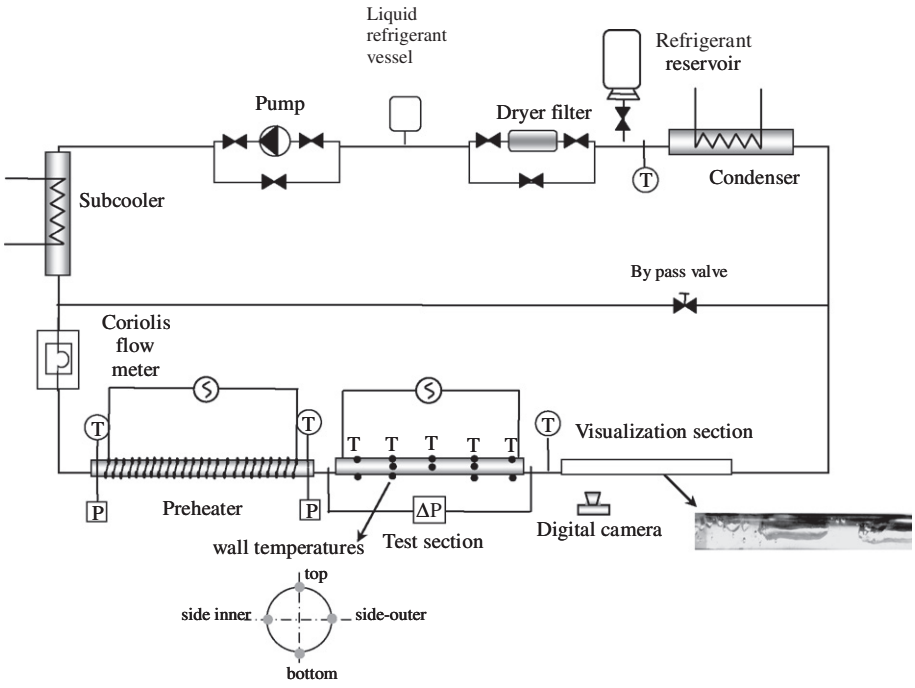

Fig. 1. Schematic view of the experimental facility.

a multimeter (Agilent, model 34970A), controlled by a computer via RS232 interface.

The oscillatory instabilities during the flow boiling in mini and micro channels reported in literature (e.g. [8,19]) were analyzed in the context of external wall temperature fluctuations and differential pressure fluctuations along the test section. The measured fluctuations were within the uncertainty ranges of the temperature and pressure sensors.

2.2. Measurement procedures and data reduction

2.2.1. Single phase

Before running boiling experiments, single phase tests were performed with R-134a to evaluate the heat losses in the pre-heater and test section. Assuming that the efficiency of the heat transfer process is the rate of heat transferred to the fluid divided by the electrical power input, as in Eq. (1), the efficiency of both pre-heater and test section could be determined for a set of operation conditions,

$$\eta = \frac{\dot{m}(i_{\text{out}} - i_{\text{in}})}{P} \tag{1}$$

where η is the efficiency, $\dot{m}$ the mass flow rate, i_{out} and i_{in} the outlet and inlet enthalpies, respectively, and P the electrical power input. The enthalpies were determined using measured values of pressure and temperature.

The efficiency was mass velocity and heat power dependent, decreasing with decreasing mass velocity and increasing heat power. In the pre-heater the average efficiency, η_{PH}, was around 85% and in the test section, η_{ST}, 95%. These efficiencies were considered in all calculations herein.

2.2.2. Experimental conditions

Boiling tests of R-134a in a 2.62 mm ID tube were carried out with the aim of verifying the thermal and hydraulic behavior for different refrigerant flow rates and heat fluxes. Experimental test conditions are shown in Table 1. The vapor quality condition in the entrance of test section for each test was reached by imposing different heating powers in the pre-heater.

2.2.3. Data reduction

Results from experimental data, including vapor quality, internal wall temperature, saturation temperature and the heat transfer coefficient, were calculated from measured data of refrigerant temperatures, wall temperatures in the test section, pressures, flow rate, heat flux and geometrical parameters. The thermodynamic properties of R-134a were obtained from REFPROP software [20].

The heat transfer coefficient calculation supposed the following considerations:

- Heat transfer in the axial direction can be neglected.
- Volumetric heat generation, and hence heat flux, is uniform along the tube in the test section.
- Pressure drop from the saturation point to outlet pressure is a linear function of tube length.

The vapor quality in the test section inlet was calculated from energy balance in the pre-heater, using Eqs. (2) and (3), as follows:

$$i_{i-TS} = \frac{q_{PH}\eta_{PH}}{\dot{m}} + i_{i-PH} \tag{2}$$

$$X_{i-TS} = \frac{i_{i-TS} - i_f}{i_{fg}} \tag{3}$$

where i_{i-TS} is the test section inlet enthalpy, i_{i-PH}, is the pre-heater inlet enthalpy, q_{PH}, is the pre-heater heat rate, η_{PH} is the pre-heater heat exchange efficiency, $\dot{m}$ is the mass rate, X_{i-TS} is the vapor quality in the entrance of test section, and i_f and i_{fg} are the liquid enthalpy and latent heat of vaporization, respectively. The enthalpies were estimated by pressure measurements downstream and upstream the section.

The local heat transfer coefficient, h, was determined according to the Newton's cooling law:

$$h = \frac{q''\eta_{ST}}{T_{wi} - T_{\text{sat}}} \tag{4}$$

where q'' is the imposed heat flux, T_{wi} is the internal wall temperature and T_{sat} is the saturation temperature at a local pressure calculated by interpolation between the inlet and outlet pressures and η_{TS} is the test section heat exchange efficiency. The heat flux is calculated as the ratio between the electrical power and the internal area for the heated length. The T_{wi} was calculated assuming radial conduction through the wall, subjected to internal heat generation as given by the following equation:

$$T_{wi} = T_{wo} + \frac{\dot{q}}{4k}(r_o^2 - r_i^2) - \frac{\dot{q}}{2k} r_o^2 \ln(r_o/r_i) \tag{5}$$

where $\dot{q}$ is the volumetric heat generated, T_{wo} is the external wall temperature, k is thermal conductivity and r_o and r_i the external and internal radios, respectively.

For each axial location z along the test tube, the external wall temperature was assumed to be the average of measured temperatures around the cross section and calculated by following equation:

$$T_{wo} = \frac{T_{w,top} + T_{w,side\_outer} + T_{w,side\_inner} + T_{w,bottom}}{4} \tag{6}$$

where $T_{w,top}$ is the external wall top temperature, $T_{w,side\_outer}$ is the external wall temperature in the outer side, $T_{w,side\_inner}$ is the external wall temperature in the inner side and $T_{w,bottom}$ is the external wall bottom temperature (see Fig. 1).

The local enthalpy and vapor quality in the test section were estimated as in the pre-heating section.

2.2.4. Uncertainties analysis

The parameters uncertainties were estimated considering the instruments uncertainties and the method of expanded uncertainty, according to Moffat et al. [21].

The experimental uncertainties associated with the sensors are listed in Table 2. The maximum experimental uncertainties calculated for the heat transfer coefficient are shown in Table 3 for various experimental conditions. The uncertainty decreases with the increase in heat flux for the same mass velocity. The maximum relative uncertainty for the heat transfer coefficient ($dh_{\max}$) achieved 34.2% in the conditions of the smallest mass

Table 1
Test conditions.

Test section heat flux, q'' (kW/m^2)	5, 10, 20, 33, 47, 67, 87 and 100
Mass velocity, G (kg/m^2 s)	240, 440, 556, 740 and 930
Saturation temperature, T_{sat} (°C)	12 and 22
Pre-heater heating power, q_{PH} (W)	45–270

Table 2
Uncertainty of sensors.

Measured parameter	Uncertainty
Absolute pressure	0.31 kPa
Temperature	0.50 °C
Differential pressure	0.12 kPa
Mass velocity	0.20%

Table 3
Heat transfer coefficient uncertainty under various conditions.

G (kg/m^2 s)	q'' (W/m^2)	dh_{max} (%)
240	5	34.2
240	47	9.5
930	10	26.2
930	100	7.1

velocity $G = 240$ kg/(m^2 s) and heat flux of $q'' = 5$ W/m^2. The maximum uncertainty for the vapor quality was 2.1%.

3. Results and discussion

3.1. Heat transfer

3.1.1. Effect of heat flux

Fig. 2a and b show the effect of heat flux on the heat transfer coefficient for different mass velocities. It is possible to verify the dependence of the heat transfer coefficient on the heat flux, mainly at the low quality region ($X < 0.4$). The heat transfer coefficient increases with the heat flux increment, in accordance to other authors observations (e.g. [5,12,15]). This condition will tend to be suppressed at high vapor quality where the effect of heat flux on the heat transfer coefficient becomes lower and the coefficient decreases, as can be observed in Fig. 2b, in agreement with [14]. Fig. 2a also shows that for low mass velocity and heat flux (240 kg/(m^2 s) and 5 kW/m^2) the heat transfer coefficient is almost constant and independent of the increase in vapor quality.

3.1.2. Effect of mass velocity

The effect of mass velocity on the heat transfer coefficient is shown in Fig. 3, for $q'' = 10$ kW/m^2 and 87 kW/m^2. It is possible to observe the significant effect of mass velocity for the low heat flux

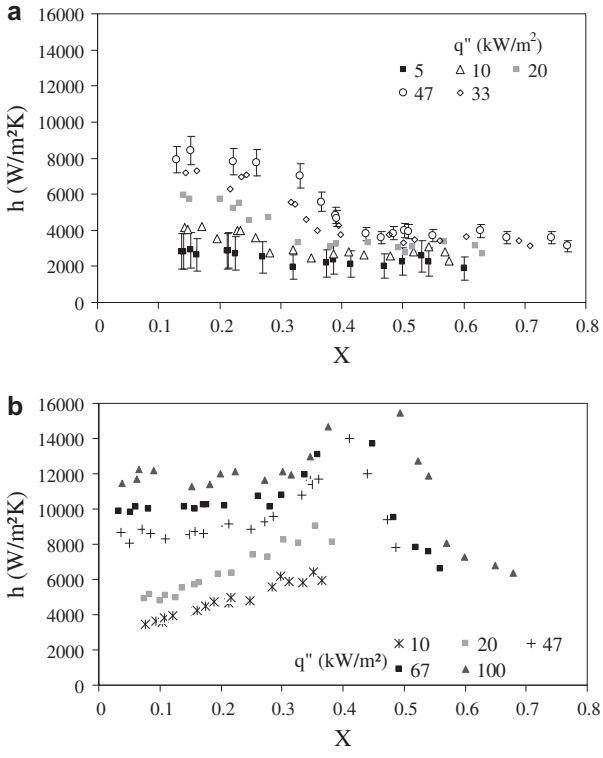

Fig. 2. Effect of heat flux on the heat transfer coefficient for different mass velocities and $T_{sat} = 22$ °C: (a) $G = 240$ and (b) $G = 440$ kg/m^2 s.

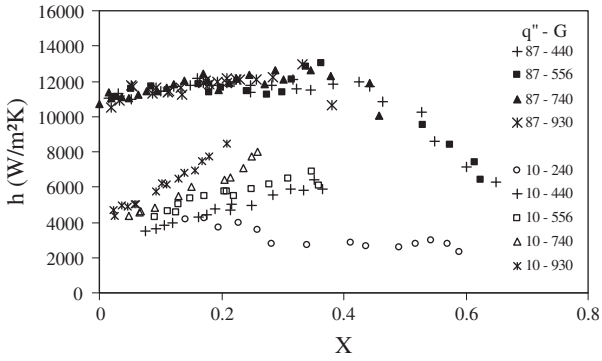

Fig. 3. Effect of mass velocity on the heat transfer coefficient for different heat fluxes and $T_{sat} = 22$ °C.

($q'' = 10$ kW/m^2). As G increases, the heat transfer coefficient also increases, except for the lowest mass velocity ($G = 240$ kg/(m^2 s)), for which the coefficient is practically constant. This results agree with those of Tibiriçá and Ribatski [17]. For higher heat flux ($q'' = 87$ kW/m^2) the heat transfer coefficient is higher and nearly independent of mass velocity. For high vapor qualities the heat transfer coefficient experiments an increase and a sudden decrease, which could indicate local occurrence of dryout, in accordance with Shiferaw et al. [10]. The decrease in the heat transfer coefficient occurs at lower qualities for higher mass velocities.

In the previous results it was possible to verify that the heat transfer coefficient behavior depends on the heat flux, mass velocity and quality range, and is related to the flow patterns.

Preliminary analyses were carried out with respect to measurements of the wall temperature distribution along to the tube perimeter (as indicated in the Fig. 1). The results of the heat transfer coefficient at the four locations (top, bottom, side_outer and side_inner) are shown in Fig. 4a and b.

In Fig. 4a, for the lower mass velocity ($G = 240$ kg/(m^2 s)) and heat flux ($q'' = 10$ kW/m^2) the heat transfer coefficient at the top is found to be the lowest up to $X = 0.3$, compared with the coefficients at the sides and the bottom. Probably this is due to vapor in contact with the upper portion of the tube. The results in Fig. 4a also show some oscillations in the distribution that can be related to the unsteadiness of liquid near the interface of gas and liquid. The change of the heat transfer coefficient distribution above $X = 0.3$ may correspond to the location where the transition of the flow pattern occurs. For the case of higher mass velocity ($G = 440$ kg/(m^2 s)) and heat flux ($q'' = 67$ kW/m^2), Fig. 4b, unlike in Fig. 4a, the heat transfer coefficient increases along the tube and its distribution around the periphery is different. Near the inlet, the top heat transfer coefficient is higher than bottom and sides and it may be indicative of intermittent flow. This condition is inverted to quality over 0.3, where the bottom heat transfer coefficient is higher and it should correspond to semi-annular flow.

Fig. 5 also complements this analysis showing some pictures obtained during tests. The flow patterns of dispersed bubbles and elongated bubbles are only found in very high mass velocities and low qualities. The patterns soon develop to intermittent (slug or semi-annular) and annular flows. Pamitran et al. [22] found the same patterns for R-134a and mini channel comparing their data with Wojtan et al. [23] flow pattern map.

3.1.3. Effect of saturation temperature

Fig. 6 illustrates the effect of the saturation temperature on the heat transfer coefficient for $G = 440$ kg/(m^2 s) and $q'' = 10$ kW/m^2. Two temperatures were tested, 12 °C and 22 °C. The heat transfer coefficient increased with increasing saturation temperature. The authors Tibiriçá and Ribatski [17] have come to the same

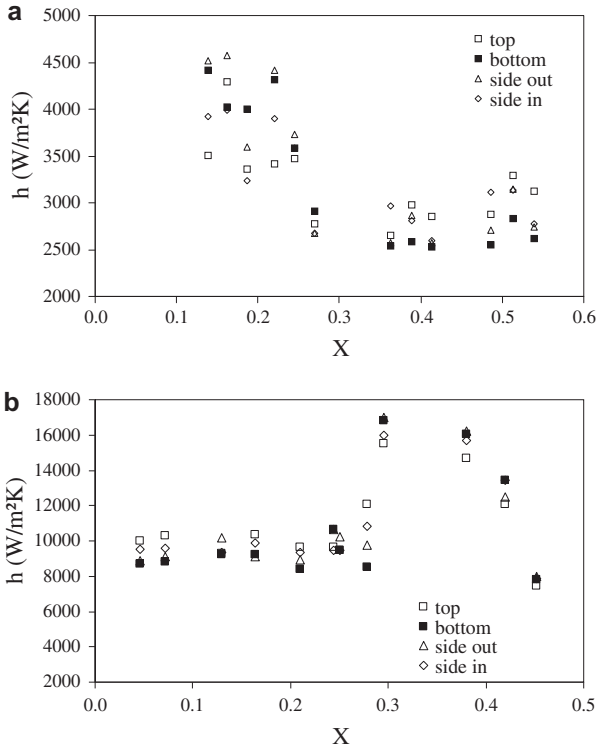

Fig. 4. Heat transfer coefficient distribution along to the tube diameter for T_{sat} = 22 °C and different mass velocity and heat flux: (a) G = 240 kg/m^2 s and q'' = 10 kW/m^2; (b) G = 440 kg/m^2 s and q'' = 67 kW/m^2.

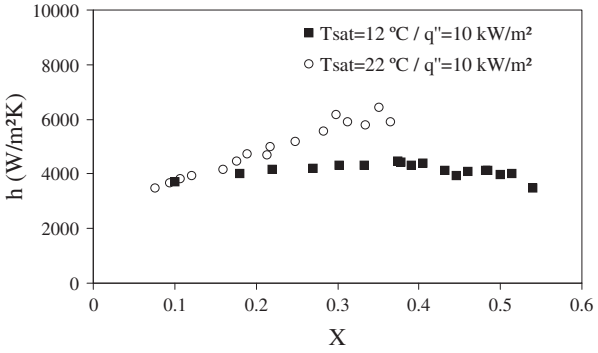

Fig. 6. Effect of saturation temperature on heat transfer coefficient for G = 440 kg/(m^2 s) and q'' = 10 kW/m^2.

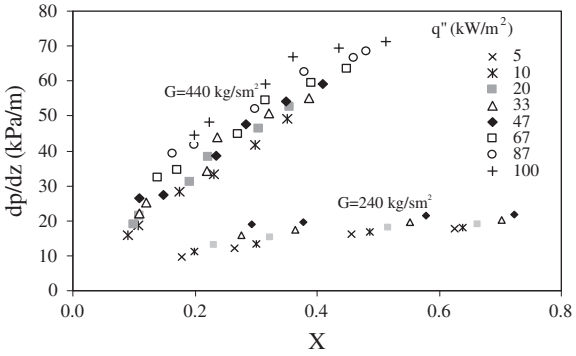

Fig. 7. Pressure drop variation: effect of heat flux for G = 440 and 240 kg/m^2 s.

conclusion employing higher saturation temperatures, and in that case the saturation temperature dependence was less pronounced.

3.2. Pressure drop

The total pressure drop was measured in the test section for different heat fluxes and mass velocities. The local pressure drop, dp/dz, was calculated assuming the pressure as a linear function of tube length. As it can be seen in Fig. 7, the local pressure drop increases with the vapor quality and mass velocity, as expected, and one can detect some influence of heat flux for higher mass velocity. Decreasing mass velocity, G = 240 kg/(m^2 s), the pressure drop tends to remain almost constant and the dependence on heat flux is rather small.

The total two-phase flow pressure drop consists of two components: acceleration and frictional. The acceleration component results from flow acceleration due to specific volume enhancement in evaporation. This component was calculated using the homogeneous correlation for void fraction and subtracted from the measured total pressure drop to give the frictional pressure drop component, dp/dz_f.

A high dependence of frictional pressure drop on mass velocity is possible to be verified in Fig. 8. This trend is due to the dependence of pressure drop on the volumetric flow rate, which is directly increased by the increase of vapor quality and mass velocity. Similar trends were presented by Ould Didi et al. [24] for refrigerants flow in macro tubes of 10.92–12 mm and by Tran et al. [25], for small channels. In the same figure, the effect of heat flux is pointed out. Despite the expectation that the heat flux would not affect the frictional pressure drop component, the experimental results show small variations in frictional pressure drop with heat flux. The trend of the current experimental results is similar to that shown by Pamitran et al. [22].

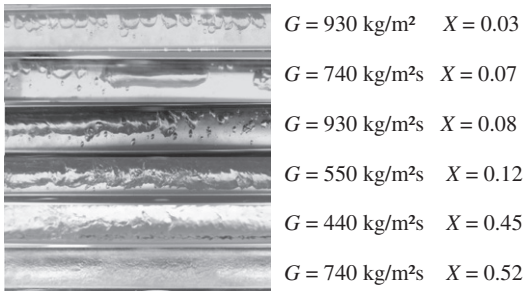

Fig. 5. Images of flow patterns during boiling tests under different conditions and T_{sat} = 22 °C.

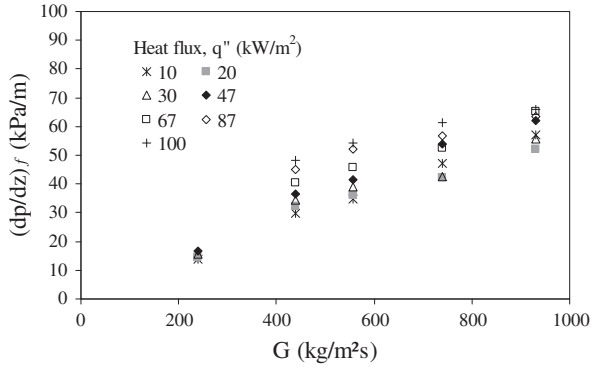

Fig. 8. Frictional pressure drop variation: effect of mass velocity for various heat fluxes and T_{sat} = 22 °C.

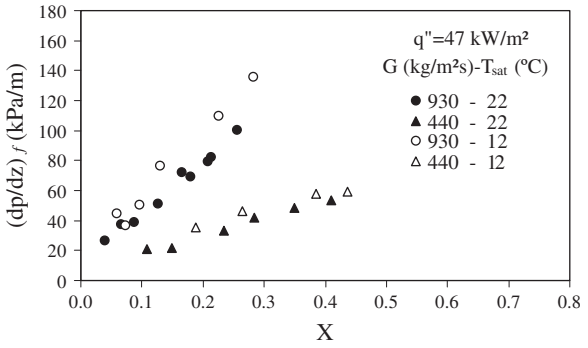

Fig. 9. Effect of saturation temperature on frictional pressure drop for mass velocity, $G = 930$ and 440 kg/m^2 s and heat flux, $q'' = 47$ kW/m^2.

Fig. 9 illustrates the effect of saturation temperature in pressure drop. A lower saturation temperature results in a slightly higher pressure drop. This pressure effect is in qualitative agreement with large-tube results and this result can be explained by the variations of the physical properties density and viscosity with temperature, manly the liquid-to-vapor density ratio.

4. Comparison between the experimental data and the predictive methods

4.1. Heat transfer coefficient

In this section, the experimental results of this work are compared to results predicted by existing correlations for the same operational conditions. The selected correlations are the ones of Kandlikar and Balasubramanian [11], Saitoh et al. [26] and Choi et al. [14]. These correlations were developed for mini channels and are summarized in Table 4, which includes the description of the tested geometries and experimental conditions. They all comprise the fluid R-134a and the ranges of heat flux and mass velocity of the present work.

The comparisons between the experimental heat transfer coefficient, h_{exp}, and the predicted heat transfer coefficient, h_{pred}, for different models are shown in the Fig. 10a–c. The performance of the models was evaluated on the basis of two statistical criteria: root mean square error (RMSE), which indicates the dispersion of the regression; and mean bias error (MBE), which indicates the variation of the calculated values with respect to measured ones.

Table 5 depicts the evaluation results. The best correlation for $T_{sat} = 22$ °C is the Kandlikar and Balasubramanian [11], with the lowest average error (0.08%) and less dispersion of data (23.31%), falling within the 35% error band (Fig. 10a). However, this correlation cannot predict well the data for $T_{sat} = 12$ °C, reaching 80.28% of dispersion. The model proposed by Saitoh et al. [26] under predicted the data, but indicates dispersion in the band error of 35% for the two saturation temperatures (Fig. 10b). Almost the same results were found with the Choi et al. [14] correlation whose values of MBE and RSME are quite similar to temperature of 22 °C, but for 12 °C showed higher dispersion and overestimation of the data (Fig. 10c).

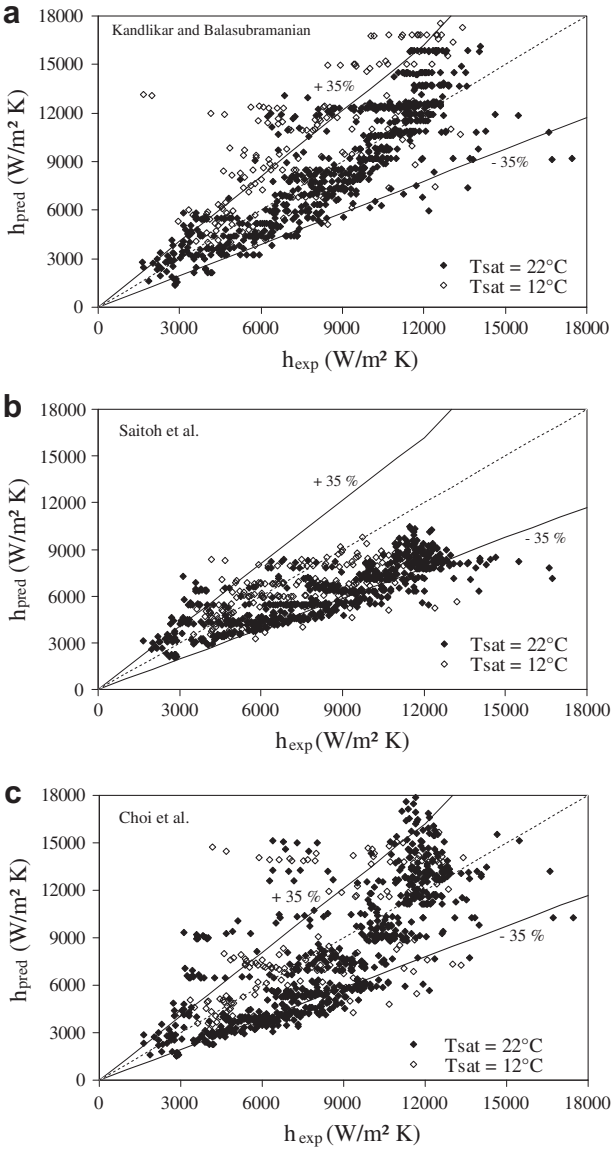

Fig. 10. Experimental versus predicted heat transfer coefficient by different correlations: (a) Kandlikar and Balasubramanian [11], (b) Saitoh et al. [26] and (c) Choi et al. [14].

4.2. Frictional pressure drop

The experimental data of frictional pressure drop were compared with three correlations: Friedel [27], Müller-Steinhagen and Heck [28] and Tran et al. [25]. The first two correlations used a large data base of frictional pressure gradients in macro-scale to adjust "separated" flow models for predicting the two-phase flow multiplier for horizontal flows in circular tubes. Müller-Steinhagen and Heck [28] suggested a simple and convenient correlation, which was developed for a variety of fluids and flow conditions. The third correlation was the one proposed by Tran et al. [25] for small scale channels.

Table 4
Correlations for flow boiling heat transfer characteristics.

Study/correlation	Fluid	D (mm)	G (kg/m^2 s)	q'' (kW/m^2)
Kandlikar and Balasubramanian [11]	R-113, R-134a R-123, R-141b, Water	0.19–2.92	50–570	10–40
Saitoh et al. [26]	R-134a	0.5–11	150–300	12–20
Choi et al. [14]	R-134a, R-22,CO_2	1.5–3.0	200–600	0.5–9.1

Table 5
Deviations of previous correlations for flow boiling heat transfer coefficient, *h*.

Errors/correlation	Kandlikar and Balasubramanian [11]		Saitoh et al. [26]		Choi et al. [14]	
T_{sat} (°C)	22	12	22	12	22	12
MBE (%)	0.08	0.36	−20.75	−7.26	−4.73	8.49
RMSE (%)	23.31	80.28	32.79	24.32	37.86	45.22

Table 6
Deviations of the frictional pressure gradient, comparison between the present data and the correlations.

Deviation (%)	Friedel [27]	Müller-Seinhagen and Heck [28]	Tran et al. [25]
MBE	−53.75	−61.78	−44.51
RMSE	54.29	62.07	45.95

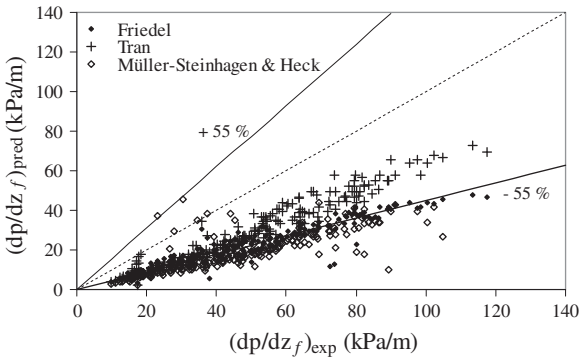

Fig. 11. Comparison between the experimental pressure drop results and the prediction methods.

These authors introduced confinement effects of a bubble within a small channel on the frictional pressure drop and the correlation was based on the Chishom B-coefficient method [29]. The model considered measurements carried out for refrigerants R-134a, R-12 and R-113 in two circular tubes of 2.46 and 2.92 mm inside diameter, pressures ranging from 138 to 856 kPa, mass velocities and heat fluxes were 33–832 kg/m^2 s and 2.2–129 kW/m^2, respectively.

The comparison is given in Table 6, through the RSME and MBE errors, and in Fig. 11.

The Tran et al. [25] correlation was the best fitted to the experimental data, with a dispersion of 45.95%, although the model underpredicted the data at −44.51%. The Müller-Seinhagen and Heck [28], followed by Friedel [27], showed larger errors (see Table 6 and Fig. 11). In general it is expected, because the correlations for macro-scale fail to predict small-channel response. The pressure drop is strongly influenced by the dynamics of the growing bubbles and flowing in a narrow confined space. According to Ribatski et al. [30], in a large tube the bubbles grow and flow along the tubes going through different flow regimes without restriction, unlike the smaller channels where the coalesced bubbles are confined, elongated, and slide over a thin liquid film as they flow downstream. Therefore, the greater pressure drop in a small channel may be due to additional friction related to the deformed/elongated bubble movement. In addition, it is expected in small diameter tubes that the effect of surface tension may become more pronounced while the influence of gravity may become less important and consequently stratified flows are rarely observed. Thus, the correlations developed for macro-scale may not extrapolate well to the micro-scale.

5. Final remarks

Experimental results for the flow boiling of R-134a in a horizontal mini channel under the variation of mass velocity, heat flux, saturation temperature and vapor quality were presented. The behavior of the local heat transfer coefficient and frictional pressure drop were investigated and the following conclusions could be drawn from this study:

1. In the low quality region, it was possible to observe a significant influence of heat flux on the heat transfer coefficient. In the high vapor quality region, for high mass velocities, this influence tended to vanish, and the coefficient decreased.
2. The influence of mass velocity in the heat transfer coefficient was detected in most tests for a threshold value of vapor quality, which was higher as the heat flux increased. For higher heat flux the heat transfer coefficient was nearly independent of mass velocity.
3. The preliminary analyses of the local heat transfer coefficient distribution along to the tube perimeter showed changes in this coefficient that may correspond to the location where the transition of the flow pattern occurs for different operational conditions and quality. The flow visualization contributed to this analysis allowing indentified patterns like bubbles and elongated bubbles, for high mass velocities and low qualities, intermittent (slug or semi-annular) and annular.
4. The frictional pressure drop increased with the increase in vapor quality and mass velocity, as expected, and one could detect some influence of the heat flux for higher mass velocities. A lower saturation temperature resulted in a slightly higher pressure drop.
5. Predictive models for heat transfer coefficient in mini channels were evaluated and the calculated coefficient agreed well with measured data within a range 35% for saturation temperature of 22 °C. The Kandlikar and Balasubramanian [11] gave the best predictions. For frictional pressure drop, the Tran et al. [25] mini channel model was the best fitted to the experimental data and the correlations developed for macro-scale not extrapolated well the current data. The statistical deviations of the best methods still remain quite large with respect to the accuracy desired for reliable thermal design of evaporators and condensers.

Acknowledgements

The authors gratefully acknowledge MCT/CNPq for the financial support, under contract 476843/2006-5. The authors Zinani, F. and Macagnan, M.H. acknowledge CNPq for financial support. The author Kunsler, N. acknowledges the undergraduate scholarships from FAPERGS and CNPq.

References

[1] T.N. Tran, M.W. Wambsganss, D.M. France, Small circular- and rectangular-channel boiling with two refrigerants, International Journal of Multiphase Flow 22 (1996) 485–498.
[2] G.M. Lazarek, S.H. Black, Evaporative heat transfer, pressure drop and critical heat flux in a small vertical tube with R-113, International Journal of Heat and Mass Transfer 25 (1982) 945–960.

[3] W. Qu, I. Mudawar, Flow boiling heat transfer in two-phase micro-channel heat sinks – I. Experimental investigation and assessment of correlation methods, International Journal of Heat and Mass Transfer 46 (2003) 2755–2771.
[4] Y.-Y. Yan, T.-F. Lin, Evaporation heat transfer and pressure drop of refrigerant R-134a in a small pipe, International Journal of Heat and Mass Transfer 41 (1998) 4183–4194.
[5] S. Lin, P.A. Kew, K. Cornwell, Two-phase heat transfer to a refrigerant in a 1 mm diameter tube, International Journal of Refrigeration 24 (2001) 51–56.
[6] A.M. Jacobi, J.R. Thome, Heat transfer model for evaporation of elongated bubble flows in microchannels, Journal of Heat Transfer 124 (2002) 1131–1136.
[7] J.R. Thome, V. Dupont, A.M. Jacobi, Heat transfer model for evaporation in microchannels. Part I: presentation of the model, International Journal of Heat and Mass Transfer 47 (2004) 3375–3385.
[8] L. Consolini, Convective boiling heat transfer in a single microchannel, Ph.D. Thesis, École Polytechnique Federale de Lausanne, Switzerland, 2008, 98p.
[9] D. Shiferaw, X. Huo, T.G. Karayiannis, D.B.R. Kenning, Examination of heat transfer correlations and a model for flow boiling of R134a in small diameter tubes, International Journal of Heat and Mass Transfer 50 (2007) 5177–5193.
[10] D. Shiferaw, T.G. Karayiannis, D.B.R. Kenning, Flow boiling in a 1.1 mm tube with R134a: experimental results and comparison with model, International Journal of Thermal Sciences 48 (2009) 331–341.
[11] S.G. Kandlikar, P. Balasubramanian, An extension of the flow boiling correlation to transition, laminar, and deep laminar flows in minichannels and microchannels, Heat Transfer Engineering 25 (2004) 86–93.
[12] C. Vlasie, H. Macchi, J. Guilpart, B. Agostini, Flow boiling in small diameter channels, International Journal of Refrigeration 27 (2004) 191–201.
[13] M.W. Wambsganss, D.M. France, J.A. Jendrzejczyk, T.N. Tran, Boiling heat transfer in a horizontal small-diameter tube, Journal of Heat Transfer 115 (1993) 963–972.
[14] K.-I. Choi, A.S. Pamitran, C.-Y. Oh, J.-T. Oh, Boiling heat transfer of R-22, R-134a, and CO_2 in horizontal smooth minichannels, International Journal of Refrigeration 30 (2007) 1336–1346.
[15] S. Saitoh, H. Daiguji, E. Hihara, Effect of tube diameter on boiling heat transfer of R-134a in horizontal small-diameter tubes, International Journal of Heat and Mass Transfer 48 (2005) 4973–4984.
[16] S.G. Kandlikar, Fundamental issues related to flow boiling in minichannels and microchannels, Experimental Thermal and Fluid Science 26 (2002) 389–407.
[17] C.B. Tibiriçá, G. Ribatski, Flow boiling heat transfer of R134a and R245fa in a 2.3 mm tube, International Journal of Heat and Mass Transfer 53 (2010) 2459–2468.
[18] C.L. Ong, J.R. Thome, Flow boiling heat transfer of R134a, R236fa and R245fa in a horizontal 1.030 mm circular channel, Experimental Thermal and Fluid Science 33 (2009) 651–663.
[19] A.E. Bergles, S.G. Kandlikar, On the nature of critical heat flux in microchannels, Journal of Heat Transfer 127 (2005) 101–107.
[20] M.L. Huber, E.W. Lemmon, M.O. McLinden, NIST Standard Reference Database 23: Reference Fluid Thermodynamic and Transport Properties – REFPROP, in, National Institute of Standards and Technology, Standard Reference Data Program, Gaithersburg, 2007.
[21] R.J. Moffat, Describing the uncertainties in experimental results, Experimental Thermal and Fluid Science 1 (1988) 3–17.
[22] A.S. Pamitran, K.-I. Choi, J.-T. Oh, P. Hrnjak, Characteristics of two-phase flow pattern transitions and pressure drop of five refrigerants in horizontal circular small tubes, International Journal of Refrigeration 33 (2010) 578–588.
[23] L. Wojtan, T. Ursenbacher, J.R. Thome, Investigation of flow boiling in horizontal tubes: part I – a new diabatic two-phase flow pattern map, International Journal of Heat Mass Transfer 48 (2005) 2955–2969.
[24] M.B. Ould Didi, N. Kattan, J.R. Thome, Prediction of two-phase pressure gradients of refrigerants in horizontal tubes, International Journal of Refrigeration 25 (2002) 935–947.
[25] T.N. Tran, M.C. Chyu, M.W. Wambsganss, D.M. France, Two-phase pressure drop of refrigerants during flow boiling in small channels: an experimental investigation and correlation development, International Journal of Multiphase Flow 26 (2000) 1739–1754.
[26] S. Saitoh, H. Daiguji, E. Hihara, Correlation for boiling heat transfer of R-134a in horizontal tubes including effect of tube diameter, International Journal of Heat and Mass Transfer 50 (2007) 5215–5225.
[27] L. Friedel, Improved friction pressure drop correlations for horizontal and vertical two phase pipe flow, European Two-Phase Flow Group Meeting, Paper E2, 1979, Ispra, Italy.
[28] H. Müller-Steinhagen, K. Heck, A simple friction pressure drop correlation for two-phase flow in pipes, Chemical Engineering Processing: Process Intensification 20 (1986) 297–308.
[29] D. Chisholm, Pressure gradients due to friction during the flow of evaporating two-phase mixtures in smooth tubes and channels, International Journal of Heat and Mass Transfer 16 (1973) 347–358.
[30] G. Ribatski, L. Wojtan, J.R. Thome, An analysis of experimental data and prediction methods for two-phase frictional pressure drop and flow boiling heat transfer in micro-scale channels, Experimental Thermal and Fluid Science 31 (2006) 1–19.